Title

Utility and reproducibility of 3-dimensional printed models in pre-operative planning of complex thoracic tumors

Journal

Journal of Surgical Oncology, 116(3)

ISSN

8756-0437

Authors

George, Elizabeth
Barile, Maria
Tang, Anji
et al.

Publication Date

2017-09-01

DOI

10.1002/jso.24684

Peer reviewed

HHS Public Access

Author manuscript

J Surg Oncol. Author manuscript; available in PMC 2018 September 01.

Published in final edited form as:

J Surg Oncol. 2017 September ; 116(3): 407–415. doi:10.1002/jso.24684.

Utility and Reproducibility of 3-Dimensional Printed Models in Pre-Operative Planning of Complex Thoracic Tumors

Elizabeth George, MD[1,2], **Maria Barile, MD**[1], **Anji Tang, BS**[2], **Ory Wiesel, MD**[3], **Antonio Coppolino, MD**[3], **Andreas Giannopoulos, MD**[2], **Steven Mentzer, MD**[3], **Michael Jaklitsch, MD**[3], **Andetta Hunsaker, MD**[1], and **Dimitrios Mitsouras, PhD**[2]

[1]Division of Thoracic Imaging, Department of Radiology, Brigham and Women's Hospital, Harvard Medical School, Boston, MA 02115

[2]Applied Imaging Science Lab, Department of Radiology, Brigham and Women's Hospital, Harvard Medical School, Boston, MA 02115

[3]Division of Thoracic Surgery, Brigham and Women's Hospital, Harvard Medical School, Boston, MA 02115

Abstract

Background and Objectives—3D-printed models are increasingly used for surgical planning. We assessed the utility, accuracy and reproducibility of 3D printing to assist visualization of complex thoracic tumors for surgical planning.

Methods—Models were created from pre-operative images for three patients using a standard radiology 3D workstation. Operating surgeons assessed model utility using the Gillespie scale (1=inferior to 4=superior), and accuracy compared to intraoperative findings. Model variability was assessed for one patient for whom two models were created independently. The models were compared subjectively by surgeons and quantitatively based on overlap of depicted tissues, and differences in tumor volume and proximity to tissues.

Results—Models were superior to imaging and 3D visualization for surgical planning (mean score=3.4), particularly for determining surgical approach (score=4) and resectability (score=3.7). Model accuracy was good to excellent. In the two models created for one patient, tissue volumes overlapped by >86.5%, and tumor volume and area of tissues ≤1mm to the tumor differed by <15% and <1.8cm^2, respectively. Surgeons considered these differences to have negligible effect on surgical planning.

Conclusion—3D printing assists surgical planning for complex thoracic tumors. Models can be created by radiologists using routine practice tools with sufficient accuracy and clinically negligible variability.

Keywords

3D printing; superior sulcus tumor; mediastinal invasion; chest wall invasion; thoracic oncology; thoracic surgery

Address correspondence to: Dimitrios Mitsouras, Ph.D. and Andetta Hunsaker, M.D., Department of Radiology, Brigham and Women's Hospital, 75 Francis Street, Boston, MA 02115, dmitsouras@alum.mit.edu, Tel: 617-732-6291; Fax: 617-264-5245.

Introduction

Accurate staging of complex thoracic tumors increasingly relies on computed tomography (CT) and magnetic resonance imaging (MRI). Meticulous staging involves assessment of nodal stations and invasion/abutment of vital structures such as the vasculature. Newer MRI sequences can distinguish between tumor abutting or invading vascular structures, and MR neurography can assess brachial plexus integrity. However, images are not always available in the operating room and the spatial information that can be conveyed on a 2-dimensional screen is limited. 3D printing is a novel technology increasingly used in clinical practice to produce physical models of a patient's anatomy from imaging. These anatomical models have been used to assist procedure planning and intra-operative guidance in diverse surgical scenarios [1,2]. By offering a greater understanding of spatial relationships prior to the initiation of a surgical procedure, this technology may assist the surgeon to select the best surgical approach, identify high-risk areas, anticipate complications, and the need for consultation of other surgical specialties [1]. These models can also be utilized as a teaching tool for both patients and surgeons in training [1].

Most clinically-acquired cross-sectional imaging, including CT and MRI can be used to produce 3D-printed models. The process involves, first, segmentation of the tissues of interest from the acquired cross-sectional images in order to precisely separate individual components of the chest anatomy from surrounding structures. The radiologist performs this by identifying the tumor margins, vessels, and other adjacent vital structures. This process is already performed in clinical practice to produce 3D visualizations that are often provided to surgical teams. Second, a specialized computer algorithm translates the tissues segmented by the radiologist into a set of surfaces that enclose the 3D volume occupied by each tissue. These surface models (stored in so-called stereolithography or STL files) can be directly printed with a variety of 3D printers using various materials ranging from plastics to metals [1,3]. Clinical application of 3D printing technology is hindered by the lack of expertise on the part of the radiologists and the general lack of interdisciplinary collaboration. As a collaborative effort, our institution has established a clinical 3D printing service using a desktop stereolithography printer and standard 3D radiology workstation software that caters to multiple surgical specialties on an as-needed basis.

A major source of requests to this service has been for patients with complex thoracic tumors that involve the lung apex, mediastinum, or chest wall. These are surgically challenging as they often invade vital structures such as the mediastinal vessels, brachial plexus, ribs, sternum, and vertebral bodies. Two such difficult pathologies for which 3D printing has already been explored to assist anatomic visualization are superior sulcus tumors and synovial sarcoma of the chest wall [4] [5,6]. Superior sulcus tumors have traditionally been associated with poor prognosis. However, implementation of a trimodality approach (neoadjuvant chemoradiation therapy followed by surgery) and advances in surgical technique have improved rates of complete resection and long-term survival [7–9]. Synovial sarcoma of the chest wall is a rare aggressive tumor particularly affecting young adults. It has modest chemosensitivity and is associated with high recurrence rate [10,11]. Prognosis in these patients remains poor even with trimodality therapy [12].

The purpose of this work was to establish the utility, accuracy and reproducibility of 3D printing technology as an aid to anatomic visualization for these pathologies in a routine clinical practice setting, and to identify those aspects of surgical planning that can potentially benefit from its use.

Materials and Methods

Patients & Imaging

Three patients with biopsy-proven complex thoracic cancers (n=2 superior sulcus adenocarcinoma; and n=1 locally recurrent synovial sarcoma) were included in this institutional review board-approved study. Case 1 was a 70 year old female with an 8 cm left upper lobe lung adenocarcinoma (T3N1M0). Case 2 was a 70 year old female with a 4.6 cm right upper lobe adenocarcinoma (T4N0M0) invading the mediastinum. Both these patients had completed neoadjuvant chemoradiation therapy. Case 3 was a 39 year old male with history of metastatic right anterior chest wall synovial sarcoma status post chemotherapy, metastatectomy, radiation therapy and multiple chest wall resections and reconstruction, who newly presented with three pleural-based enhancing masses suspicious for recurrence. One of these pleural-based masses was located in the right lung apex in close proximity to the subclavian vessels.

All three patients had undergone routine pre-operative diagnostic contrast enhanced CT performed at end inspiration from the thoracic inlet to the adrenal glands using 64 or 128 slice multidetector CT scanners (Aquilion 64, Toshiba Medical Systems, Tochigi-ken, Japan, and, Somatom Definition, Siemens Healthcare, Erlangen, Germany) at 120 kVp with automatic tube current modulation and a quality reference of 200 mAs. A total of 50–100 mL of Omnipaque 350 (GE Healthcare, Chicago, IL) was administered intravenously via a power injector (Medrad, Pittsburgh, PA). Standard chest CT images were reconstructed for interpretation at a slice thickness of 3 mm to reduce effects from volume averaging. 3D reconstructions of the CT images were performed by a trained technologist under radiologist supervision using a commercial radiology 3D workstation (Vitrea 6.7, Vital Images Inc, Minnetonka, MN) as routine at our institution. For Case 3, pre-operative imaging also included chest wall MRI at 3 Tesla (Magnetom Trio, Siemens Healthcare, Erlangen, Germany), before and after administration of 8.5 ml of Gadavist (Bayer Healthcare, Whippany, NJ).

3D Printing

3D printed models were generated using all available pre-operative images. No additional CT or MR images were acquired or reconstructed for this process. The images were segmented using the same commercial radiology 3D workstation software (Vitrea 6.7, Vital Images Inc, Minnetonka, MN) as used for 3D visualization. Segmentation was performed semi-automatically by a radiology resident (4 years experience) who identified the margins of each individual tissue to separate the individual components of the chest anatomy (Figure 1). The tumor, adjacent ribs and upper vertebrae, pulmonary vasculature, thoracic aorta and arch vessels, and systemic veins of the neck were segmented from the preoperative CT of each patient. In the case of synovial sarcoma, tumors were additionally segmented in the

contrast-enhanced MRI images, where tumor enhancement assists separation from chest wall soft tissue and changes from prior surgery and reconstruction. Each segmented tissue was exported directly into STL file format from the radiology workstation and imported into FDA-approved 3D-printing post-processing software (3-matics, Materialise NV, Belgium).

Post-processing is a semi-automatic process used to optimize STL files for 3D printing [1]. This process was performed by a medical physicist (12 years experience) and included smoothing to remove surface irregularities, trimming the automatically segmented tissues to the area of interest (e.g., removing the contralateral ribs and cardiac chambers), hollowing of the model to reduce printing time and material usage, and the addition of connecting elements (rods) so that anatomically isolated tissues (e.g., aorta and ribcage) could remain together and maintain their spatial relationships after printing (Figure 1). The post-processed STL files of each tissue were printed on a desktop stereolithography printer (Form1+, Formlabs, Somerville, MA) using different-colored rigid acrylics (photopolymers), and assembled into the complete model by snap-fitting the connecting elements.

3D Model Clinical Utility & Accuracy Assessment

The 3D-printed models were provided to the surgical team before the procedure and were available in the operating room (OR) for use during the procedure. The operating surgeons (n=6) subjectively assessed 3D model utility for surgical planning and the accuracy of tumor spatial relationship to surrounding structures. Utility was assessed compared to the standard-of-care at our institution (review of imaging and 3D visualization) using a questionnaire (Table 1) partly based on the ordinal Gillespie score scale (1=inferior information gathered from model; 2=similar information gathered in similar time; 3=superior in that similar information was assimilated more rapidly; and 4=superior in that additional conceptual information was obtained [13]). Accuracy was assessed with respect to intra-operative findings on an ordinal scale of 1 to 4 (1=poor to 4=excellent; Table 1).

3D Model Inter-Observer Variability Assessment

Inter-observer variability of the technique was assessed by creating a second 3D-printed model for one of the superior sulcus tumor patients included in the study. For the second model, images were segmented independently by a second radiology faculty member (medical physicist with 12 years experience in image segmentation). Post-processing of tissue STLs and 3D printing were performed identically (i.e., using identical parameters) for both models in order enable direct comparison of depicted tissue volumes. Following the surgery, operating surgeons compared the accuracy of each model in depicting spatial relationships with respect to intra-operative findings, as well as their utility for surgical planning based on the questionnaire described in the previous section.

To elucidate any subjective differences between the two models noted by the surgeons, a set of quantitative metrics were additionally used to compare the two models. First, two metrics were used to quantify spatial relationships of the tumor mathematically, by comparing tumor volume and tumor proximity to surrounding tissues depicted in each model. Proximity was calculated using the extent (defined by surface area) of each tissue (e.g., systemic arteries) that was ≤1 mm away from the tumor. The 1 mm cutoff was arbitrarily chosen as a limit that

may alter the surgeon's perception of abutment/invasion of tissues by the tumor. A third metric was used to quantify the similarity of each tissue depicted in the two models. This metric, termed the Dice similarity index[14], summarizes the difference in size, shape and overlap between two STL models created for a single tissue (e.g., as created by two different radiology software operators). It is calculated as $S=(2\times V_{OL})/(V_A+V_B)$, where V_{OL} is the volume of the two STLs that spatially overlaps, and V_A and V_B are the volume of each STL [14]. For example, if the tumor is identically depicted (i.e., size and shape) as well as in the identical spatial location in both models, the STL volumes exactly overlap, and S=1. Conversely, if the tumor is depicted identically (size/shape) in both models, but its location differs by e.g., half the tumor size in one model due to discordant radiologic interpretation as to tumor location, only half the STL volumes overlap, and S=0.5.

Results

The tumor, the thoracic aorta and supra-aortic vessels, and the ipsilateral subclavian vein that were crucial to surgical planning were successfully 3D-printed for both superior sulcus adenocarcinoma cases. The models additionally included the ipsilateral 1^{st}–3^{rd} or 4^{th} ribs, upper thoracic vertebrae, proximal pulmonary vasculature, bilateral brachiocephalic veins, and the superior vena cava [SVC] (Figures 2, 3). The model in one case readily demonstrated the bulky nature of the tumor, filling the thoracic inlet and destroying large portions of the left first and second ribs, and adhering to the left subclavian artery and separate from the subclavian vein (Figure 2). For this case, considering the extensive chest wall invasion, a posterior approach was selected for left upper lobectomy with en bloc resection of 1st, 2nd and 3rd ribs, mediastinal lymphadenectomy, and lysis of adhesions of the left subclavian artery. For the second case, an anterior approach was preferred for right upper lobectomy with en bloc resection of the first rib.

In the third case, the three pleural based masses, Gortex mesh and prior surgical material, plus part of the right hemidiaphragm abutting one of the masses that were crucial to surgical planning were successfully 3D-printed. The model also included the 1^{st}–6^{th} ribs, aorta and supraaortic vessels, ipsilateral subclavian and brachiocephalic veins, and SVC (Figure 4). The model demonstrated close relationship of the apical mass to the subclavian vessels and the basal mass to the Gortex mesh and right hemidiaphragm (Figure 4). The patient underwent right anterior thoracotomy, resection of the three pleural-based masses, partial chest wall resection, omental graft interposition, and reconstruction of the anterior chest wall.

3D Model Clinical Utility & Accuracy

Surgeons reported that they referenced the models both before and during surgical dissection, occasionally to extensively. Overall, they considered the models to be highly accurate and of moderate to significant benefit for surgical planning, with a mean Gillespie score of ≥3 (superior to imaging and 3D visualization) for five of six questions (Table 1). The lowest mean score (2.5, i.e., equivalent to marginally better than review of imaging) was given for guiding instrumentation selection. All six surgeons reported that the models provided additional information for determining the surgical approach that was not

otherwise appreciated by review of imaging and 3D visualization (mean score=4). Three surgeons felt the models led to minimal (n=2) or moderate (n=1) decrease in OR time, and three were uncertain of any effect.

3D Model Inter-Observer Variability

Both operating surgeons of the patient for whom two models were created noted differences in how the models depicted tumor relationship to vessels and bones. One surgeon noted one model was more detailed, while the second noted that one model more accurately depicted tumor proximity to the 1st rib and subclavian artery with respect to intraoperative findings. Although for that patient removal of the tumor en bloc with the 1st rib and dissection off the subclavian artery were noted to be the most difficult parts of the procedure, both surgeons felt that despite differences, both models were equivalently useful for planning the procedure. Quantitative metrics confirmed the surgeon's impressions. The area of tissues closer than 1 mm to the tumor differed the most for the great vessels and bone between models (1.17 and 1.8 cm^2, respectively; Table 2, Figure 5). The volume of the tumor depicted in the two models was 19.4 ml and 22.4 ml, respectively. Overlap of tissues between models was lowest for the tumor (Dice index = 86.5%), and was high (Dice index>90%) for the arteries and veins (Table 2).

Discussion

In most cases of thoracic malignancy, routine CT and/or MR imaging with or without 3D reconstruction adequately demonstrates pathology. Nonetheless, both CT and MRI scans are limited by the spatial information that can be conveyed on a 2-dimensional computer screen. In complex cases of lesions invading mediastinal and chest wall structures and in superior sulcus tumors, review of imaging may fall short of answering critical surgical questions, even when 3D visualizations are provided. Our study suggests that in these cases, physical models of the anatomy produced by 3D printing may assist surgeons in visualizing the anatomy, providing a net benefit for surgical planning.

Reports in the medical literature suggest that 3D-printed models benefit surgical planning, multidisciplinary discussion, guidance during surgery, and patient education [1] [15] [2,3]. However, only a single study to date has systematically evaluated the utility of 3D-printed models in assisting surgical planning for oncologic cases [15]. In that study, of 19 surgeons who used a total of 52 models of tumors throughout the body, 94% considered them very helpful for treatment planning, and 71% felt they improved the surgical approach. To our knowledge, 3D-printed models specific to thoracic tumors have been reported for two patients with Pancoast tumors [5,6], a pediatric patient with primary mediastinal synovial sarcoma invading the SVC [16], a patient with an ectopic mediastinal thymoma [17], a patient with a pectoralis minor muscle spindle cell neoplasm [5], and a patient with a cardiac schwannoma [18]. Benefits reported for these cases include better understanding of tumor relationship to surrounding normal tissues, helping to avoid resecting uninvolved structures, and enhancing the likelihood of complete resection. One difficulty in adopting the technology described in all the above studies is that they have used either research [5,16] or

engineering-oriented [2,6] 3D printing software that is unfamiliar and/or unavailable to most radiologists.

Our study aimed to systematically assess whether 3D models created using standard radiology tools already in place to generate 3D visualizations in a routine practice setting are useful, accurate, and reproducible for pre-operative planning in complex thoracic malignancy. This information will be useful for the future evaluation of any clinical benefits of this technology, such as improved patient outcomes or reduction of healthcare costs. Our results suggest that 3D-printed models for this indication are feasible using standard radiology images, software and workflows. Surprisingly, despite their experience in understanding tumor relationship to surrounding structures, surgeons found these models to be superior to review of images and 3D visualizations in assisting them for surgical planning. Excluding instrumentation selection, more than half of surgeon responses (18 of 30) indicated that models provided additional relevant information not otherwise recognized from review of imaging findings, and all surgeons agreed that 3D-printed models provided additional information relevant for selecting the surgical approach. For superior sulcus tumor resection, an anterior approach offers better vascular access and control than a posterior approach, at the cost of rendering the posterior paraspinal dissection more difficult. In contrast, a posterior approach allows excellent access to the 1^{st}–3^{rd} ribs and adjacent thoracic vertebrae and their transverse processes [19,20]. In the case of multifocal recurrence of synovial sarcoma in the setting of prior chest wall reconstruction, the 3D model enabled the selection of a targeted approach with extension of the prior anterior thoracotomy to assess and excise the three pleural-based foci of tumor with adequate margins, while reducing perioperative morbidity.

Beyond utility and accuracy, reproducibility of a technology is a major factor that can be detrimental to its application. Two models created for one patient differed in how they depicted tumor relationships to vessels and bones. The differences were perceptible to surgeons, but had no significant impact on model utility for surgical planning. Variability in the models is introduced primarily by the radiology software operator in the process of segmenting the images, and less frequently due to intrinsic inaccuracies involved in the 3D printing process [21]. Quantitative metrics suggest that the bulk of model differences perceived by surgeons where due to how each software operator delineated tumor and bone tissue boundaries. Tumor depiction disagreed the most between models (lowest Dice similarity index of 86.5%). The discrepancy appeared to be in tumor size rather than shape and/or location. Specifically, tumor volume differed by 14.4% between models (19.4 vs 22.4 ml). In this case, the maximum Dice similarity index possible is 86.6%, and would be achieved if the tumor depicted by one model fully inscribed that depicted in the other model. Any further disagreement in its shape and/or location would have necessarily led to a lower Dice index than that observed (86.5%).

Difficulty in segmenting the tumor is due to similar CT numbers with surrounding apical soft tissue. Thus, careful review of tumor segmentation by the interpreting radiologist appears necessary to ensure model accuracy. In the synovial sarcoma case, MRI was used synergistically with CT to distinguish enhancing tumor from chest wall muscle. Combining the higher spatial resolution of CT with the higher tissue contrast resolution of MRI can help

increase the accuracy of tumor delineation. MRI is also commonly used in evaluation of superior sulcus tumors. However, there are many contraindications to MRI including implanted devices. Although none of the two superior sulcus tumor patients in our study had a pre-operative MRI, if available, it can be used in conjunction with the CT as was done for the synovial sarcoma case.

The variability observed for bone between models (second-lowest agreement, Dice similarity index of 88.4%) was unexpected given that osseous structures have much higher CT number than surrounding soft tissues, which simplifies segmentation. In the case we used to assess model variability, segmentation of bone was complicated by an overlap of CT numbers between the 1st rib and dense contrast-enhanced neck veins. Thus to ensure accuracy of bones depicted in the 3D-printed models, we believe it is important to either include a non-contrast CT acquisition, or, if such an acquisition is not routinely performed, to alternatively perform the intravenous CT contrast injection in the contralateral side to that of the pathology.

Limitations of this study include the small number of patients and the lack of clinical outcomes. Larger studies are required to determine whether the technology offers objective clinical benefits. Based on our results, we believe the logistics of establishing a clinical 3D printing service, including time required to produce the models and the purchase and maintenance costs of a 3D printer, to be the main limitations in using the technology. Our models were simple, using only color without texture (e.g., mechanical properties) to convey distinct tissues. Desktop 3D printers that can use color, such as the one we used, are sufficiently low-cost ($3000–5000) to support a practice-based 3D printing service. 3D printing materials exist and more are being developed specifically for medical applications that can additionally convey tissue texture to enable for example surgical simulation. These materials nonetheless require a larger equipment investment (>$200,000) [1]. Finally, outside companies can print STL files generated in-hospital at reasonable cost, which can simplify the process and avoid equipment investments.

A limitation of this technology is the labor-intensive image segmentation required to create the models, particularly given the number and complexity of tissues involved in these challenging cases. Despite using a 3D workstation familiar to our practice that helped minimize this time, each case still required roughly 10 hours to produce printable models. Nonetheless, our results suggest that staff trained in standard radiology software can perform the image segmentation and post-processing required to produce these models, with the interpreting radiologist’s role limited to oversight and verification of accuracy. Future 3D printing software and hardware improvements will likely yield significant time savings [1]. Furthermore, new techniques are being actively developed to enhance the utility of the technology, for example creating models that convey not only the anatomy, as done here, but also physiology, for example by incorporating PET-CT findings such as the hypermetabolic areas of a tumor, or pre-and post-chemoradiation therapy tumor dimensions [6]. A final potential limitation of the technology is that surgeons using the models did not feel they reduced operating room (OR) time. This is in contrast to reports in other surgical specialties, which suggest the introduction of 3D printed models can yield a 28–30 min (12–13%)

reduction in OR time [22,23]. A reduction in OR time of 20–30 min is possible in our study, but may not have been perceived as the procedures were lengthy.

In summary, the use of 3D printing in complex surgical oncology is increasing, aided by advances in printing technology and radiology software. We assessed the utility and reproducibility of 3D printing from routine radiology imaging and workflows in a small cohort of patients with encouraging results. The technology was superior to the current standard of care in assisting surgeons with visualizing the anatomy for surgical planning. Interdisciplinary collaboration between radiology and thoracic surgery in identifying complex cases that could benefit from this technology may enhance the expert care provided to patients.

Acknowledgments

Grant sponsor: National Institute of Biomedical Imaging and Bioengineering, grant number: EB015868; **Grant Sponsor**: Vital Images, a Toshiba Medical Systems Company.

References

1. Mitsouras D, Liacouras P, Imanzadeh A, et al. Medical 3D Printing for the Radiologist. Radiographics. 2015; 35:1965–1988. [PubMed: 26562233]
2. Matsumoto JS, Morris JM, Foley TA, et al. Three-dimensional Physical Modeling: Applications and Experience at Mayo Clinic. Radiographics. 2015; 35:1989–2006. [PubMed: 26562234]
3. Giannopoulos A, Steigner M, George E, et al. Cardiothoracic Applications of 3D Printing. Journal of Thoracic Imaging. 2016 In press.
4. Gillaspie, E., Arun, J., Dickinson, K., et al. [October 30, 2016] Minimally Invasive Approach to Pancoast Tumor Using 3D Printing. 2015. Available from: http://www.ctsnet.org/article/minimally-invasive-approach-pancoast-tumor-using-3d-printing
5. Kim MP, Ta AH, Ellsworth WAt, et al. Three dimensional model for surgical planning in resection of thoracic tumors. International journal of surgery case reports. 2015; 16:127–129. [PubMed: 26453940]
6. Gillaspie EA, Matsumoto JS, Morris NE, et al. From 3-Dimensional Printing to 5-Dimensional Printing: Enhancing Thoracic Surgical Planning and Resection of Complex Tumors. The Annals of thoracic surgery. 2016; 101:1958–1962. [PubMed: 27106426]
7. Shen KR, Meyers BF, Larner JM, et al. Special treatment issues in lung cancer: ACCP evidence-based clinical practice guidelines (2nd edition). Chest. 2007; 132:290S–305S. [PubMed: 17873175]
8. Tamura M, Hoda MA, Klepetko W. Current treatment paradigms of superior sulcus tumours. European journal of cardio-thoracic surgery: official journal of the European Association for Cardio-thoracic Surgery. 2009; 36:747–753. [PubMed: 19699106]
9. Jeannin G, Merle P, Janicot H, et al. Combined treatment modalities in Pancoast tumor: results of a monocentric retrospective study. Chinese clinical oncology. 2015; 4:39. [PubMed: 26730751]
10. Duran-Mendicuti A, Costello P, Vargas SO. Primary synovial sarcoma of the chest: radiographic and clinicopathologic correlation. J Thorac Imaging. 2003; 18:87–93. [PubMed: 12700482]
11. Hung JJ, Chou TY, Sun CH, et al. Primary synovial sarcoma of the posterior chest wall. The Annals of thoracic surgery. 2008; 85:2120–2122. [PubMed: 18498838]
12. Braham E, Aloui S, Aouadi S, et al. Synovial sarcoma of the chest wall: a case report and literature review. Annals of translational medicine. 2013; 1:9. [PubMed: 25332954]
13. Gillespie JE, Isherwood I, Barker GR, Quayle AA. Three-dimensional reformations of computed tomography in the assessment of facial trauma. Clinical radiology. 1987; 38:523–526. [PubMed: 3665350]

14. Frolich AM, Spallek J, Brehmer L, et al. 3D Printing of Intracranial Aneurysms Using Fused Deposition Modeling Offers Highly Accurate Replications. AJNR American journal of neuroradiology. 2016; 37:120–124. [PubMed: 26294648]
15. Matsumoto JS, Morris JM, Rose PS. 3-Dimensional Printed Anatomic Models as Planning Aids in Complex Oncology Surgery. JAMA oncology. 2016; 2:1121–1122. [PubMed: 27533241]
16. Krauel L, Fenollosa F, Riaza L, et al. Use of 3D Prototypes for Complex Surgical Oncologic Cases. World journal of surgery. 2016; 40:889–894. [PubMed: 26541866]
17. Akiba T, Nakada T, Inagaki T. A three-dimensional mediastinal model created with rapid prototyping in a patient with ectopic thymoma. Annals of thoracic and cardiovascular surgery: official journal of the Association of Thoracic and Cardiovascular Surgeons of Asia. 2015; 21:87–89.
18. Son KH, Kim KW, Ahn CB, et al. Surgical Planning by 3D Printing for Primary Cardiac Schwannoma Resection. Yonsei medical journal. 2015; 56:1735–1737. [PubMed: 26446661]
19. Panagopoulos N, Leivaditis V, Koletsis E, et al. Pancoast tumors: characteristics and preoperative assessment. Journal of thoracic disease. 2014; 6(Suppl 1):S108–115. [PubMed: 24672686]
20. Spaggiari L, D'Aiuto M, Veronesi G, et al. Anterior approach for Pancoast tumor resection. Multimedia manual of cardiothoracic surgery: MMCTS. 2007; 2007 mmcts 2005 001776.
21. George E, Liacouras P, Rybicki FJ, Mitsouras D. Measuring and Establishing the Accuracy & Reproducibility of 3D-Printed Medical Models. Radiographics. 2016 In press.
22. Weinstock P, Prabhu SP, Flynn K, et al. Optimizing cerebrovascular surgical and endovascular procedures in children via personalized 3D printing. Journal of neurosurgery Pediatrics. 2015:1–6.
23. Yang M, Li C, Li Y, et al. Application of 3D rapid prototyping technology in posterior corrective surgery for Lenke 1 adolescent idiopathic scoliosis patients. Medicine. 2015; 94:e582. [PubMed: 25715261]

Synopsis

Accurate and reproducible 3D-printed physical models of the anatomy of patients with thoracic tumors that invade adjacent vital structures in the superior sulcus, mediastinum, and chest wall can be created with standard radiology workflows. When used to assist anatomic visualization, the 3D-printed models subjectively enhance nearly all aspects of surgical planning.

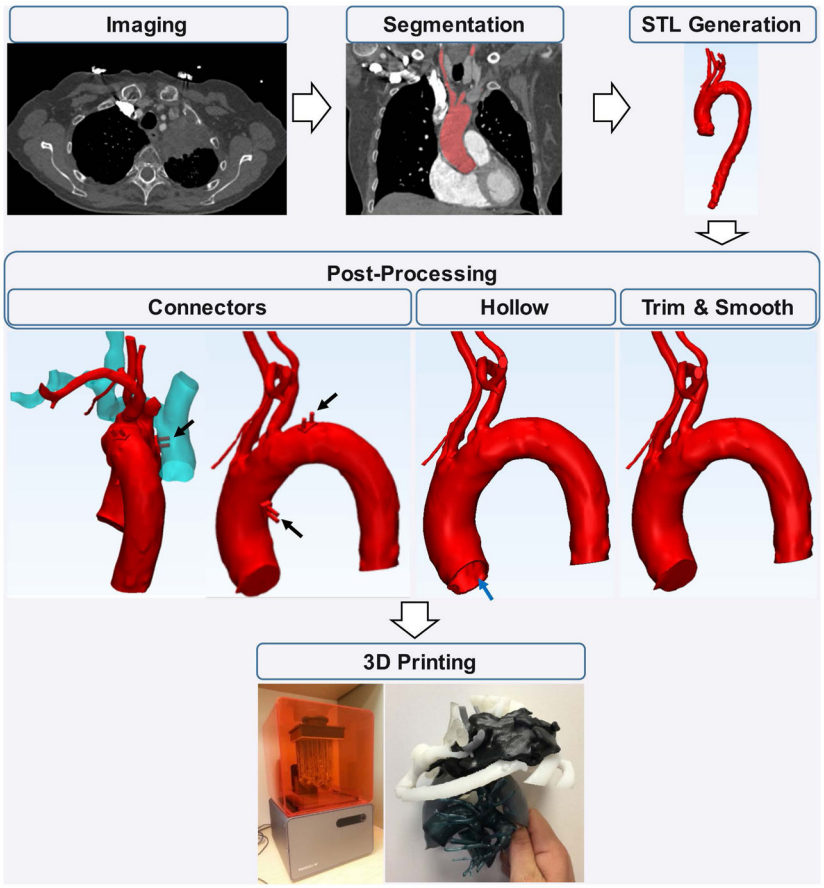

Figure 1.

Workflow of generation of 3D-printed models. Segmentation of aorta and supra-aortic vessels in contrast-enhanced CT is used to create an STL surface that encloses the (segmented) arterial blood pool. The STL surface is typically post-processed, including smoothing and trimming to the region of interest, hollowing to reduce printing material and time (blue arrow), and addition of connectors (black arrows) to adjacent structures, followed by 3D printing.

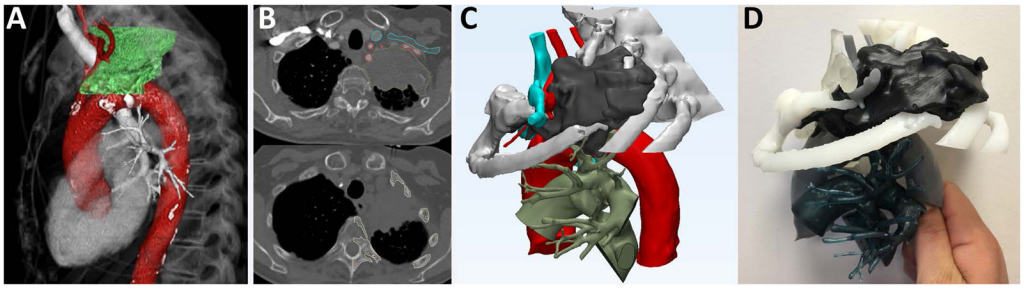

Figure 2.

(**A**) Standard 3D visualization, (**B**) overlay of tumor and systemic vessel STL models on source contrast-enhanced CT acquisition, and overlay of bone segmentation on source non-contrast CT acquisition, and (C) post-processed STL model; tumor (black), systemic arteries (red), systemic veins (turquoise), pulmonary vasculature (deep green) and bones (white). Final 3D-printed model (**D**) demonstrates adherence of tumor to the subclavian artery and vertebral body, and separation from the subclavian vein.

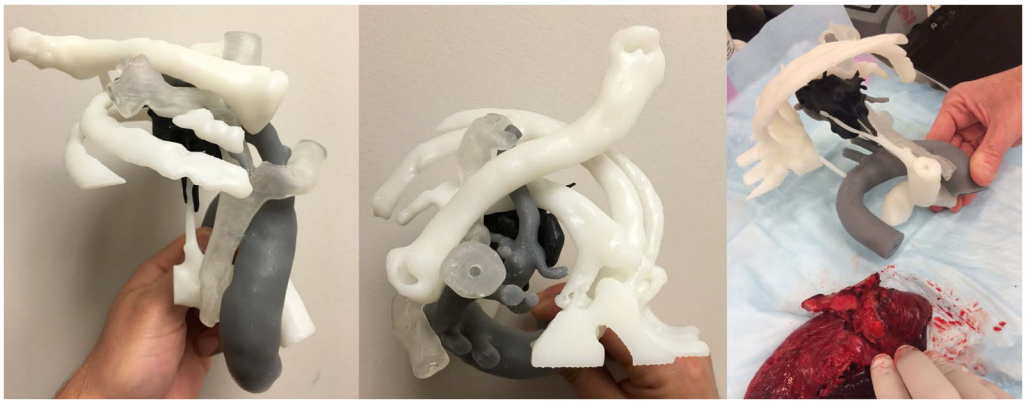

Figure 3.
3D-Printed model of Pancoast tumor (black), bone (white), systemic arteries (gray), systemic vein (translucent) and pulmonary vasculature (also white), and correlation with excised tissue in the operating room.

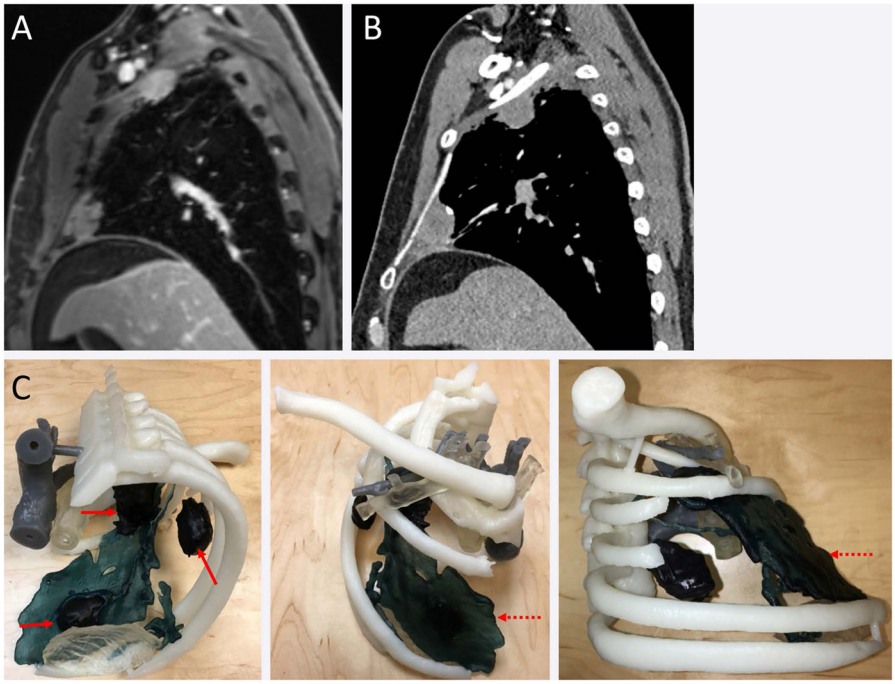

Figure 4.

Contrast enhanced MRI (A) and CT (B) demonstrate two of the three focal areas of tumor recurrence in the patient with synovial sarcoma. 3D model (C) demonstrates the relationship of the tumor (black, arrow) with the bones (white), adjacent part of the diaphragm (translucent, thick arrow), prior Gortex mesh (green, dashed arrow), systemic arteries (grey), and systemic veins (translucent).

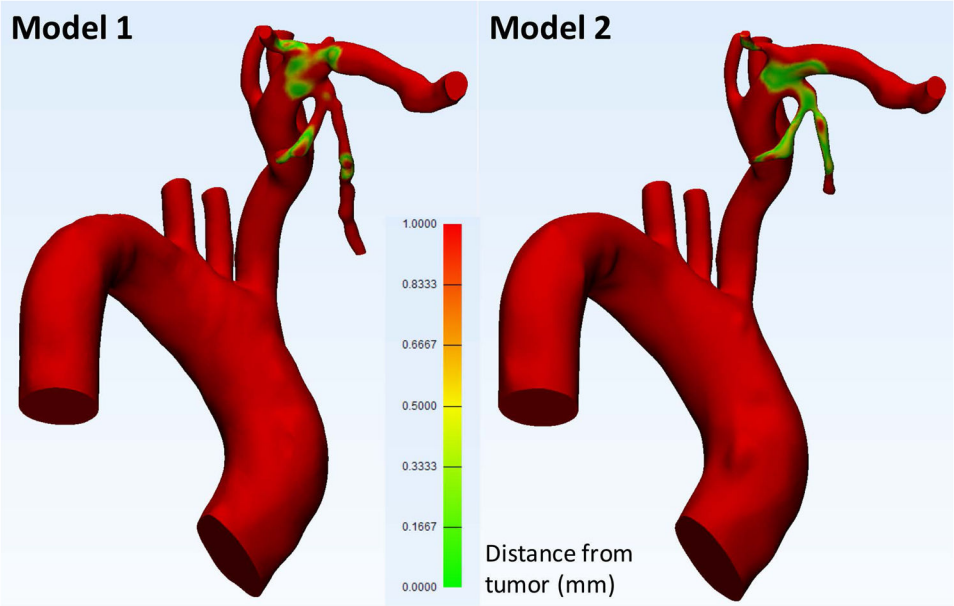

Figure 5.

Model of the aorta and branch vessels generated by two independent radiology software operators. Vessel surface color reflects the distance of the vessel to the tumor, with green closest, and red >1 mm away. Slight difference in delineation of the branches of the subclavian artery by the two operators results in a quantitative difference in the area of the branches in close proximity to the tumor.

Table 1

Questionnaire to assess the clinical utility and subjective accuracy of 3D printed models compared to standard imaging and 3D visualization. The number of surgeons operating on the three cases (n=6) in agreement with each statement are noted for each question.

Usefulness of 3D printed model as compared to standard CT images				
	Inferior	**Similar**	**Superior; similar information assimilated more rapidly**	**Superior; additional relevant information provided**
Understand relationship to vessels			3	3
Understand relationship to bones		1	2	3
Assessment of resectability			2	4
Selecting instrumentation		4	1	1
Identification of perioperative challenges and complications		1	3	2
Determining surgical approach				6
3D model accuracy compared to intra-operative findings				
	Poor	**Average**	**Good**	**Excellent**
Overall accuracy			1	5
Tumor relationship to vessels			1	5
Tumor relationship to bones			2	4
Did the model change/benefit the following?				
	Not at all	**A little**	**Moderately**	**Significantly**
Surgical planning			2	4
Surgical approach			1	5

Table 2

Measures of inter-observer variability of two 3D printed models created by two independent radiology software operators for one patient.

	Systemic arteries	Systemic veins	Bones	Pulmonary artery	Tumor
Tissue area in ≤1 mm proximity to tumor (cm^2)					
Model 1	4.43	0.77	3.98	0	N/A
Model 2	5.6	1.92	5.78	0	N/A
Difference	1.17	1.15	1.8	0	N/A
Tissue Overlap Index (Dice similarity index, %; higher is better)					
	95.6%	93.4%	88.4%	95.3%	86.5%